DOI: http://dx.doi.org/10.18273/revion.v30n1-2017003

Reducibility and catalytic behavior of $La_{0.25}Sr_{1.75}MnO_4$ Ruddlesden-Popper phase prepared by a modified Pechini method

Reducibilidad y comportamiento catalítico de la fase Ruddlesden-Popper $La_{0,25}Sr_{1,75}MnO_4$ preparada por el método de Pechini modificado

Redutibilidade e comportamento catalítico da fase Ruddlesden-Popper $La_{0,25}Sr_{1,75}MnO_4$ preparada pelo método de Pechini modificado

Reinaldo Calderón[1,2]; Susana Larrondo[2,3c]; Gilles H. Gauthier[1,4*]

[1] Grupo de Investigación en Química Estructural (GIQUE), [4]Grupo INTERFASE, Universidad Industrial de Santander, Carrera 27, Calle 9, Ciudad Universitaria, Bucaramanga, Colombia.
[2]Centro de Investigaciones en Sólidos (UNIDEF-MINIDEF-CONICET), Juan Bautista de la Salle 4397, Prov. de Buenos Aires, República de Argentina.
[3] Instituto de Investigación e Ingeniería Ambiental, Universidad de San Martín (3iA-UNSAM), Campus Miguelete, Av. 25 de mayo y Francia, San Martín, Pcia. De Buenos Aires, Argentina.

*gilgau@uis.edu.co

Fecha Recepción: 21 de septiembre de 2016
Fecha Aceptación: 21 de marzo de 2017

Abstract
Few studies have been reported concerning the use of manganite compounds $(La,Sr)_2MnO_4$ of Ruddlesden-Popper structure type as Solid Oxide Fuel Cells (SOFCs) electrode materials; in particular, on the anode side. In the present work $La_{0.25}Sr_{1.75}MnO_4$ compound was synthesized by a modified Pechini method. This prepared manganite was characterized by X-Ray Diffraction (XRD), Scanning Electron Microscopy (SEM) and its structure was analyzed into detail by refinement of recorded XRD profiles. $La_{0.25}Sr_{1.75}MnO_4$ was also subjected to a reducibility study through Temperature Programmed Reduction (TPR) and the catalytic properties for total and/or partial oxidation of methane were evaluated. Estimated values of lattice parameters in the refinement are in good agreement with those reported in the literature for various neighbored compositions of the series. The reduction of the material in diluted H_2 occurs in several stages and the decomposition starts above 800°C. In the catalytic studies, the material acts as a catalyst for total oxidation of methane even in oxygen deficient atmospheres.

Keywords: *SOFC, anode, manganite, XRD, TPR, catalytic oxidation.*

Resumen
Se han reportado pocos estudios sobre el uso de compuestos de manganeso $(La,Sr)_2MnO_4$ de estructura tipo Ruddlesden-Popper, como electrolitos de Celdas de Combustible de Óxido Sólido (SOFC), en particular como ánodos. En este trabajo el compuesto $La_{0,25}Sr_{1,75}MnO_4$ fue sintetizado por el método de Pechini modificado. Este material fue estudiado por la técnica de Difracción de Rayos X (XRD), Microscopía Electrónica de Barrido (SEM) y su estructura analizada en detalle mediante refinamiento de los patrones de difracción de rayos X. $La_{0,25}Sr_{1,75}MnO_4$ fue sometido a un estudio de Reducción a Temperatura Programada (TPR) y se evaluaron sus propiedades catalíticas para la oxidación total y/o parcial de metano. Los parámetros de celda estimados en el refinamiento son bastante próximos con los reportados en la literatura para series con composiciones cercanas. La reducción del material en H_2

Cita: Calderón R, Larrondo S, Gauthier GH. Reducibility and catalytic behavior of La0.25Sr1.75MnO4 Ruddlesden-Popper phase prepared by a modified Pechini method. rev.ion. 2017;30(1):33-43.

diluido ocurre en múltiples etapas y la descomposición comienza por encima de 800°C. En los estudios catalíticos el material actúa como catalizador para la oxidación total de metano incluso en atmósferas deficientes de oxígeno.

Palabras clave: *SOFC, ánodo, manganita, XRD, TPR, oxidación Catalítica.*

Resumo

Poucos estudos têm sido reportados sobre o uso de compostos de manganésio $(La,Sr)_2MnO_4$ de estrutura tipo Ruddlesden-Popper, como eletrólitos de Células de Combustível de Oxido Solido (SOFC), em particular como ânodos. No presente trabalho o composto $La_{0,25}Sr_{1,75}MnO_4$ foi sintetizado pelo método de Pechini modificado. O material foi estudado pela técnica de Difração de Raios-X (XRD), Microscopia Eletrônica de Varredura (SEM) e sua estrutura analisada em detalhe mediante refinamento. $La_{0,25}Sr_{1,75}MnO_4$ foi sometido a um estudo de Redução a Temperatura Programada (TPR) e foram avaliadas as propriedades catalítica para a oxidação total e/ou parcial de metano. Os parâmetros de rede estimados no refinamento são muito parecidos com os reportados na literatura para series com composições próximas. A redução do material em H_2 diluído ocorre em múltiplos estágios e a decomposição começa por cima de 800°C. Nos estudos catalíticos o material atua como catalisador para a oxidação total de metano mesmo em atmosferas deficientes de oxigeno.

Palabras-chave: *SOFC, anodo, manganita, XRD, TPR, oxidação Catalítica.*

Introduction

Solid Oxide Fuel Cells (SOFCs) major issues are related to the degradation of electrode materials as well as the electrode-electrolyte and electrode-interconnect interfaces during long-term operation or transient conditions. It makes heating or cooling procedures sometimes heavy and complex. The most widely used SOFC anode is a cermet (ceramic-metal composite) of nickel and Yttria-Stabilized Zirconia (YSZ). Ni/YSZ cermet is commonly chosen due to low cost and high chemical stability in the reducing atmosphere of the anode; furthermore, its thermal expansion coefficient is compatible with that of the YSZ electrolyte [1-3]. Nickel in the cermet anode acts as an electrocatalyst for the electrochemical oxidation of hydrogen and provides high electronic conductivity. YSZ phase provides the ionic conductivity to the anode. The material must be highly porous in order to help increasing the number of Triple-Phase Boundaries (TPB) where the reaction can take place. At the same time, the YSZ network maintains the dispersion of nickel particles and acts as a growth inhibitor of metal grains during elaboration and operation of the cell. Unfortunately, the activity of the classical cermet and the cell performance can be affected due to kinetically favored reactions such as carbon deposition when hydrocarbons are directly fed to the anode, especially at low current density or in transient conditions. Carbon formation on the nickel surface can block the TPB [4], leading to a decrease in the power efficiency of the cell. Most research aiming at overcoming the limitations of nickel-based anodes has focused on the development of alternative materials that are catalytically active for the reforming or the oxidation of hydrocarbons (directly or indirectly) and inactive for cracking reactions that lead to carbon deposition. Other problems of Ni-YSZ cermets are the irreversible losses of activity stemming from sulphur poisoning in the case of realistic fuels like Natural Gas as well as coarsening of Ni-particles in operation and redox cycling, the latter being true even in H_2/H_2O or H_2/CO atmospheres [3,5,6].

Due to their high resistance toward reducing and sulfur-containing atmospheres, perovskite compounds (of general formula ABO_3) have attracted great interest in the last decade as a possible replacement of Ni-cermets [6-8]. Most of the solids that have been considered as anode materials, like doped-$SrTiO_3$, present the classical tridimensional perovskite structure, with La^{3+} (LST) or Y^{3+} (YST) principally doping the A-site [9-12]. To improve the electrochemical performance of those materials, which is still too low to be used as a single phase anode, cation doping at the B-site of the perovskite has been considered; among the possible cations, Mn^{3+} doping [13,14] and Ga^{3+}/Mn^{n+} co-doping [15] are worth mentioning, but with limited success [16]. Actually, for the anode side, no real attention has been played to

new structure types, especially layered materials that have revealed interesting performances as a cathode component, *e.g.* oxygen vacancy ordered $REBaCo_2O_{5+}\delta$ [17] or Ruddlesden-Popper (RP) type nickelates [18-20].

Among the RP series $(AO)(ABO_3)_n$, one of great interest is the A_2BO_4(K_2NiF_4-type) structure, which consists of alternate layers along the *[001]* direction of ABO_3 perovskite and AO rock salt compounds [21], as can be seen in Figure 1. Lanthanum-strontium manganites $(La,Sr)_2MnO_4$ have the K_2NiF_4 structure type with tetragonal *I*4/*mmm* space group [22]. In this structure, every manganese atom is surrounded by six oxygen atoms forming an octahedral and the Mn-O bonds have the direction of the crystallographic axes.

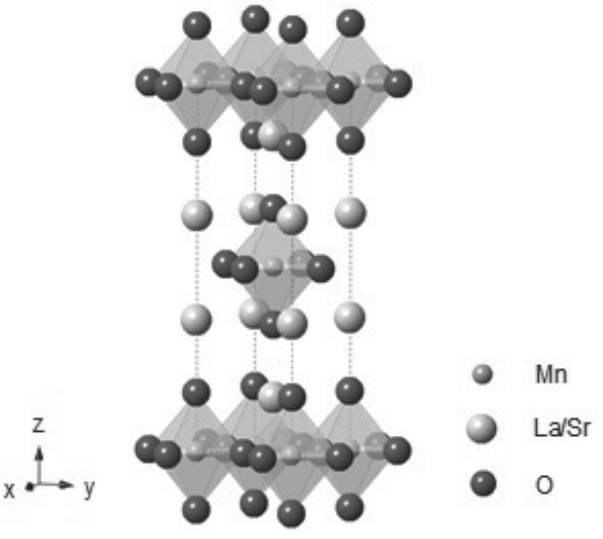

Figure 1. View of the unit cell of the $La_xSr_{2-x}MnO_4$ Ruddlesden-Popper structure.

According to literature, very few studies have been reported concerning the use of $(La,Sr)_2MnO_4$ compounds as SOFC electrode materials; in particular, on the anode side, only redox stability considerations and oxygen stoichiometry in the series are described [19,23-27]. On the other hand, and in contrast with perovskite oxides, these RP manganites have not been widely studied as oxidation catalysts (reducing atmosphere), one of the main properties to fulfil for SOFC anodes [28,29].

Considering the latter, this work was focused not only on the study of reducibility and the structural characterization of the $La_{0.25}Sr_{1.75}MnO_4$ composition, but also on the evaluation of its catalytic properties for methane oxidation.

Material and methods

A powder sample with the nominal composition $La_{0.25}Sr_{1.75}MnO_4$ was synthesized by a modified Pechini method [30], using $Sr(NO_3)_2$ (99.9965%, Alfa Aesar), $La(NO_3)_2$ (99.99%,Aldrich) and $Mn(NO_3)_2$ (99.99%, Merck) as precursors. Initially, 0.06 mole of citric acid (99%, Prolabo) were dissolved in 50ml of distilled water. Later, 0.0088 mole of $Sr(NO_3)_2$, 0.0013 mole of $La(NO_3)_2$ and 0.0050 mole of $Mn(NO_3)_2$ were added to the solution and the temperature was raised to 60°C. After getting a homogeneous solution, 0.09 mole of ethylene glycol (99%, Aldrich) was added and the temperature adjusted to 70°C, for which the polyesterification reaction occurred. Finally, the temperature was raised to 90°C to remove solvent excess and form a xerogel. The xerogel was initially treated at 350°C for 5h and then the powders were heated at 1300°C in air for 10h, at this later temperature the pure phase was formed.

Powder X-Ray Diffraction (XRD) data were collected at Room Temperature (RT) using a Bruker D8 ADVANCE X-ray Diffractometer working in Bragg-Brentano geometry with Cu $K\alpha_{1,2}$ radiations (DAVINCI design). XRD data were collected from 10º to 140º (2θ) with a step size of 0.015º. Structural refinements using the Lebail method were performed with the Fullprof Suite program [31,32]. A pseudo-Voigt function was used to model profile shapes, including the Cagliotti function variables U, V, W, the Gaussian-

Lorentzian mixing parameter η and two asymmetry parameters. The values of standard deviations were corrected according to Berar and Lelann´s description [33].

The Temperature-Programmed Reduction (TPR) technique was performed using a Micromeritics ChemiSorb 2720 chemisorption system. In each test, about 35mg of sample was probed with an H_2/Ar (5/95) reducing mixture (50cm^{3}min^{-1} at 25°C, 1atm). The temperature in the sample was increased from 30°C to 900°C using a heating ramp of 10°Cmin^{-1}, with a dwell time at 900°C of 20min. Before each TPR test, the catalyst was subjected to a degassing process in order to remove adsorbed substances. This process consisted in passing a helium gas flow of 50cm^{3}min^{-1} through the sample while heated from 30°C to 300°C, followed by a dwell time of 30min at 300°C before cooling to room temperature. For an optimal reduction profile, the weight of catalyst was selected in agreement with the recommended values of the characteristic numbers K (55-140s) and P (P<20°C) proposed by Monti *et al.* [34] and Malet *et al.* [35]. These characteristic numbers allow obtaining narrow peaks being easier to determine the position of the maximum rate and the H_2 consumption amount.

The surface analysis of the sample was examined with a Quanta 650 FEG Scanning Electron Microscope (SEM), operating in high vacuum mode using a secondary electron detector (Everhart-Thornley). A small fraction of the sample was fixed on a single specimen holder using carbon adhesive tape that was coated with gold using a Quorum Q150 TES metallizer. The sample analysis was performed with the following analytical conditions: 5−10kV of accelerating voltage and 182*μA* of beam current.

The purpose of the catalytic evaluation was to determine the activity of $La_{0.25}Sr_{1.75}MnO_4$ for partial and/or complete oxidation of methane as described by Equations 1 and 2.

$$CH_4 + \frac{1}{2}O_2 \rightarrow CO + 2H_2 \quad (1)$$

$$CH_4 + 2O_2 \rightarrow CO_2 + 2H_2O \quad (2)$$

Catalytic experiments were performed in a fixed bed lab-scale reactor, operated isothermally and at atmospheric pressure. The reactor consisted of a quartz glass tube of 12mm outer diameter and 11.2mm of inner diameter, filled with the catalytic bed. The catalyst was diluted with inert material in order to avoid the developing of hot spots, forming a bed of ~15mm in length. The reactor was placed in an oven provided with a temperature controller. The reaction temperature was monitored with a K-type thermocouple axially located in the center of the catalyst bed. Previous catalytic experiments were performed to select the operation conditions that ensure chemical reaction control [36-38]. In order to satisfy these conditions, a flow of 170mLmin^{-1} of a CH_4, O_2 and N_2 mixture was fed to a fixed-bed reactor containing 52mg of catalyst dissolved in 552mg of inert phase (catalyst/inert ratio=1/10). The inert material was a ceramic with composition unavailable. This material was previously tested in operating conditions to verify the absence of catalytic activity in the whole temperature range.

The outlet and feed stream compositions were analyzed by on-line gas chromatography using a Clarus 500 Chromatograph (Perkin Elmer), equipped with a concentric packed column (Porapak // Molecular Sieve), a thermal conductivity detector and an automatic injection valve. The amount of reaction gases was determined by calibration curves. For each data collection, several (generally 3) measurements were recorded and the final value was taken as an average. The catalyst was subjected to three different tests corresponding to the following conditions:

- Catalytic evaluation varying the reaction temperature every 50°C from 500 to 800°C to assess the catalyst activity at different temperatures. The feed molar composition was 11% of CH_4, 6% of O_2 and 83% of N_2.
- Catalytic evaluation at 745°C varying the O_2/CH_4 molar ratio from 0.04/0.094 to 0.089/0.094 to observe the catalytic behavior of the material with different feed compositions, particularly in oxygen defect conditions, that is O_2/CH_4 molar ratio lower than 1:1. The temperature was selected according to the operation ranges of intermediate temperature SOFC (IT-SOFC).
- Stability test at 745°C and a molar ratio O_2/CH_4 of 0.089/0.094, for approximately 5h to evaluate the performance of the material over time.

Results and Discussion

Structural characterization

The pure-phase formation of the material was confirmed by comparison with the PDF card number #54-1279 using the Search/Match

program [39]. A Full Pattern Matching refinement of the structural parameters was carried out by least-squares method using XRD data, according to the Le Bail procedure. The graphical result of the refinement is shown in Figure 2, in good agreement with a tetragonal cell of *I*4/*mmm* space group. The refinement quality was estimated not only by the reliability factors R_p, R_{wp} and c^2, but also by the difference between experimental and calculated patterns. In addition to reliability factors, refined cell parameters are given in Table 1. Obtained values agree well with those reported in the literature for various neighbored compositions of the series. For instance, Munnings *et al.* reported a=b ~ 3.82Å and c ~ 12.44Å and a=b ~ 3.85Å and c ~ 12.41Å for $La_{0.2}Sr_{1.8}MnO_4$ and $La_{0.4}Sr_{1.6}MnO_4$, respectively, being the materials prepared by solid state synthesis in Ar and reoxidized in air [26-40]. The morphology of $La_{0.25}Sr_{1.75}MnO_4$ sample, prepared by the modified Pechini method, has been observed by SEM imaging and is shown in Figure 3. The material presents an average grain size of about 500nm, despite the high calcination temperature (1300°C). The porous microstructure is relatively homogeneous and the grains are strongly aggregated.

Table 1. Structural data of $La_{0.25}Sr_{1.75}MnO_4$, as obtained from LeBail refinement using XRD data.

*I*4/*mmm*	a=b=3.83304(12)Å	c=12.4263(5)Å	
R_p=3.09	R_{wp}=4.25	R_{exp}=2.37	χ^2=3.22

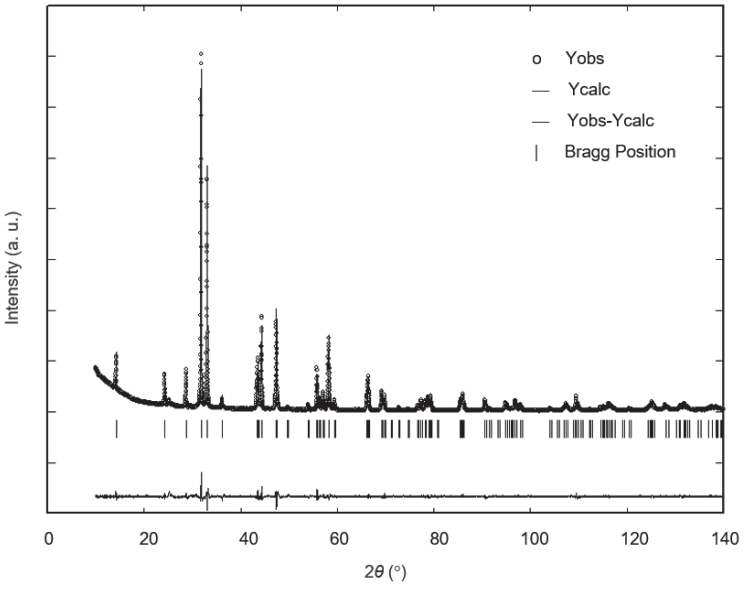

Figure 2. Graphical results of Le Bail refinement, using the DRX data of as-synthesized $La_{0.25}Sr_{1.75}MnO_4$.

Temperature-Programmed Reduction (TPR)

The reduction profile of $La_{0.25}Sr_{1.75}MnO_4$ obtained from TPR is shown in Figure 4; it presents a two-steps reduction profile, *i.e.* a low temperature peak located in the 400-600°C range and centered around 552°C, and a high temperature peak between 600°C and 800°C, centered on 697°C. TPR curve shows also an additional step beyond 850°C that is not completely finished at 900°C. Such reduction profile gives information about the reducibility of Mn^{n+} species in the material, since the A-site La^{3+} and Sr^{2+} are both non-reducible cations under the conditions of H_2-TPR [41]. TPR studies conducted on parent perovskite-type oxides $La_{1-x}Sr_xMnO_3$(x=0–0.5) have also shown two clear reduction regions (150–530 and 550–930°C), where the first region is primarily associated with reduction of $Mn^{4+}\rightarrow Mn^{3+}$ and the second region with $Mn^{3+}\rightarrow Mn^{2+}$ with a subsequent structure decomposition [42-45]. In our case, the first and second peak can be reasonably associated to $Mn^{4+}\rightarrow Mn^{3+}$ and $Mn^{3+}\rightarrow Mn^{2+}$ reduction steps, respectively, just like it proceeds for perovskite-type $(La,Sr)MnO_3$.

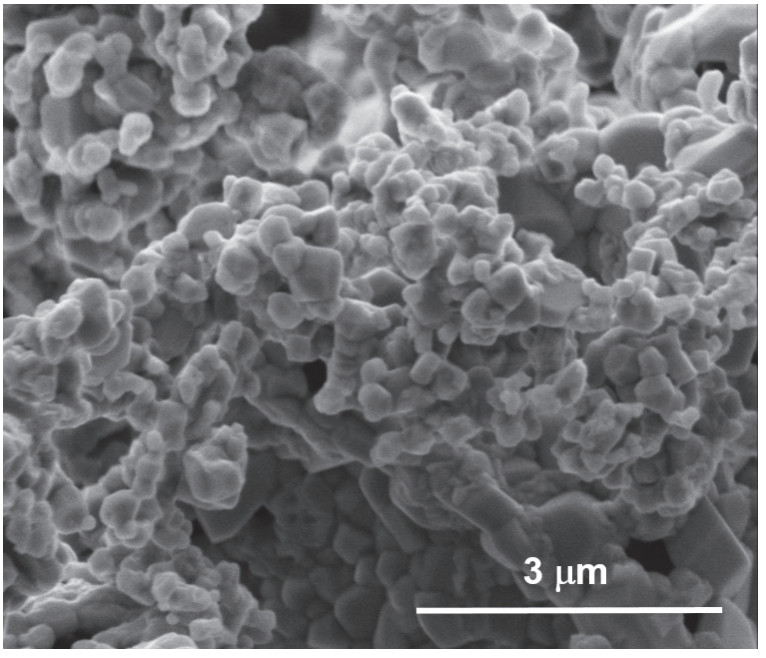

Figure 3. SEM micrograph of the material prepared ($La_{0.25}Sr_{1.75}MnO_4$).

Table 2. Hydrogen consumption in each TPR peak (mL $mmol^{-1}$) and corresponding percentage of Mn^{n+} species reduction.

Peak 1		Peak 2		Peak 3		Total
H_2	Mn (%)	H_2	Mn (%)	H_2	Mn (%)	H_2
7.7	69	0.88	7.9	0.28	2.5	8.9

The hydrogen uptake in each peak and total H_2 consumption were determined by comparing the TPR profile with a calibration function that relates H_2 consumption as a function of the reduction curve area. The results are displayed in Table 2. The nominal amount of Mn^{4+} cations present in $La_{0.25}Sr_{1.75}MnO_4$ that may be reduced in the low temperature step is theoretically 75%, if no oxygen non-stoichiometry is present initially, what has been described in literature for similar compositions $La_{0.5}Sr_{1.5}MnO_4$ and Sr_2MnO_4 prepared in air [46-47]. Reduction peaks would thus be described by Equations 3 and 4:

$$La_{0.25}Sr_{1.75}Mn_{0.25}^{III}Mn_{0.75}^{IV}O_4 + 0.375H_2 \rightarrow La_{0.25}Sr_{1.75}Mn^{III}O_{3.625} + 0.375H_2O \quad (3)$$

$$La_{0.25}Sr_{1.75}Mn^{III}O_{3.625} + \frac{1}{2}xH_2 \rightarrow La_{0.25}Sr_{1.75}Mn_x^{II}Mn_{1-x}^{III}O_{3.625-x/2} + \frac{1}{2}xH_2 \quad (4)$$

Following our hypothesis, the main (low temperature) H_2 consumption is attributed to the Mn^{4+} to Mn^{3+} reduction and the corresponding Mn equivalent is found slightly lower than theoretical assuming no oxygen vacancies (69% vs. 75%). An explanation would be the initial presence of a low oxygen vacancy concentration in the material, possibly related to the degassing process carried out in He before the TPR test. The second TPR peak, attributed to Mn^{3+} to Mn^{2+} reduction, concerns only 7.9% of the Mn atoms, *i.e.* after this second step, the material stoichiometry would be close to $La_{0.25}Sr_{1.75}Mn_{0.08}^{2+}Mn_{0.92}^{3+}O_{3.46}$. Finally, XRD analysis of the TPR residue, shown in the inset of Figure 4, confirms that $La_{0.25}Sr_{1.75}MnO_{4-\delta}$ sample began to decompose with formation of MnO, with

the conclusion that the RP manganite becomes unstable in a reducing atmosphere for temperatures higher than 800°C (during the last TPR event), what is in agreement with literature [46].

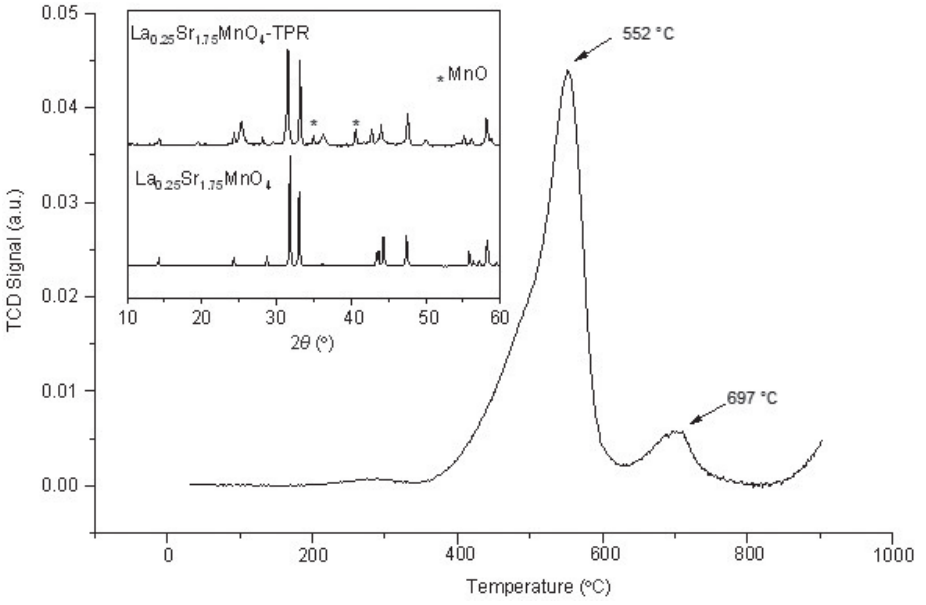

Figure 4. Temperature Programmed Reduction (TPR) profile of $La_{0.25}Sr_{1.75}MnO_4$. In inset, the XRD pattern of the sample after TPR experiment.

Another explanation to the reduction steps observed by TPR would be a symmetry- (and not Mn valence-) driven transition from original tetragonal *I*4/*mmm* space group to a monoclinic $P2_1/c$ structure with ordered oxygen vacancies, as recently described in the case of non-doped $Sr_2MnO_{4-\delta}$ [48].

In this work, the authors demonstrate that tetragonal Sr_2MnO_4 material, prepared in air and heated under dilute hydrogen flow, loses oxygen from the "MnO_2" equatorial layer above T~ 470°C with retention of tetragonal symmetry up to $Sr_2MnO_{3.70(1)}$. Further oxygen loss induces ordering of the oxygen vacancies within the equatorial layers transforming the tetragonal cell into a $P2_1/c$ monoclinic supercell. When the phase transition is complete, the refined composition of the single-phase $P2_1/c$ material is found to be $Sr_2MnO_{3.55(1)}$ and does not vary on extended heating. If the same behavior is occurring in La-doped Sr_2MnO_4, it would be interesting to understand if the origin of the second TPR peak around 700°C is not also related to the structure decomposition that was initially associated to the last H_2 consumption beyond 800°C.

Catalytic Evaluation

The catalytic tests were carried out with molar ratios of O_2:CH_4 in the range 0.4:1 to 1:1. In such conditions, the feed presents an oxygen deficiency with respect to the O_2:CH_4=2:1 stoichiometric ratio corresponding to the complete methane oxidation (Equation 2), making oxygen the limiting reactant. In Figures 5a and 5b, the oxygen conversion profiles were plotted as a function of temperature and the molar ratio O_2:CH_4, respectively. The catalytic activity of $La_{0.25}Sr_{1.75}MnO_4$ begins to become important at temperatures above 500°C (Figure 5a). This is consistent with the temperature at which the material begins to be reduced in H_2-Ar atmosphere (Figure 4). It can be observed that oxygen is completely consumed at a temperature of 800°C, which is the highest temperature of reaction being probed. According to Figure 5b, the O_2 consumption increases to near 100% when the O_2/CH_4 ratio decreases below 0.4.

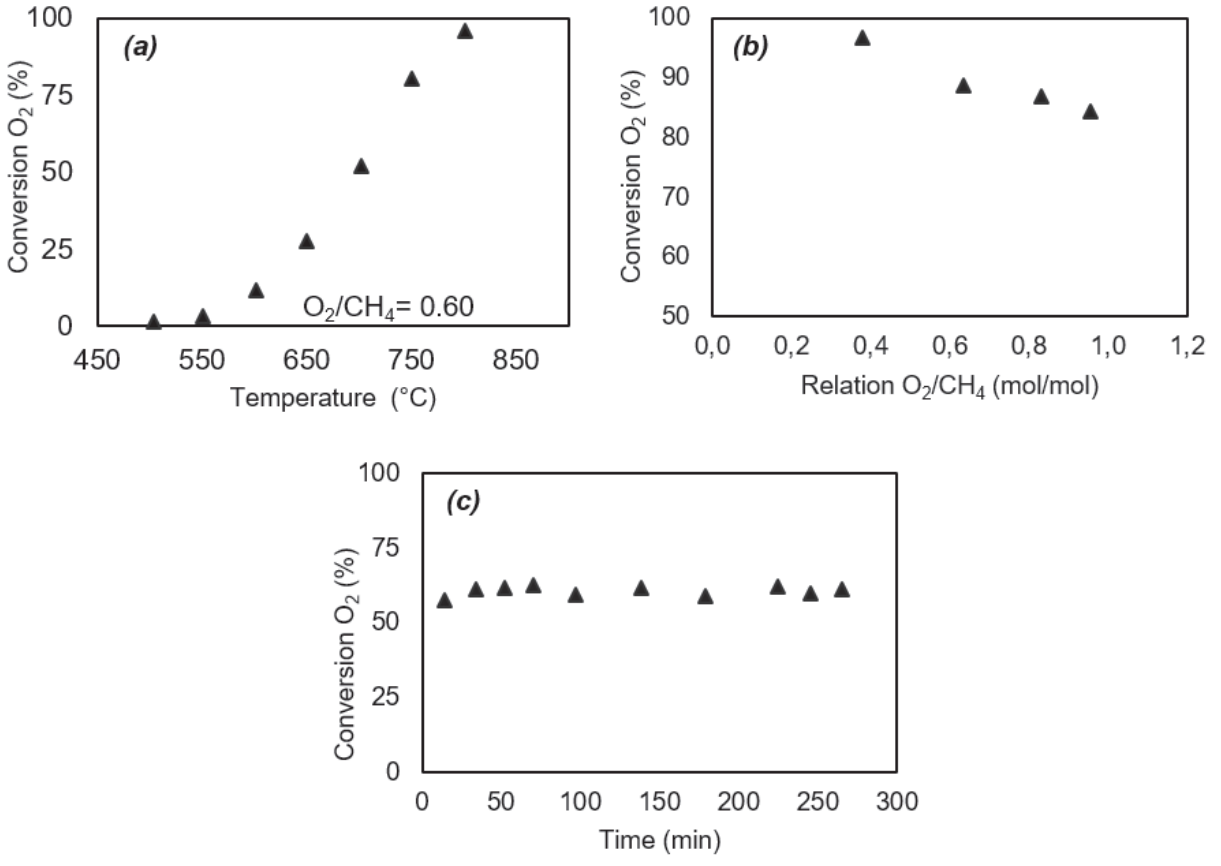

Figure 5. Catalytic activity of $La_{0.25}Sr_{1.75}MnO_4$ (a) as a function of the reaction temperature (b) as a function of the relation O_2/CH_4 at 745 °C and (c) as a function of reaction time at 745°C for a molar ratio O_2/CH_4 = 0.089/0.094 (τ= 0.31mgcatminmL^{-1}).

The only carbonaceous product that is formed is CO_2 in all catalytic tests; neither CO nor H_2 is detected at any temperature or reaction conditions. It is therefore concluded that $La_{0.25}Sr_{1.75}MnO_4$ catalyst is selective to the total methane oxidation even in oxygen-deficient conditions. Moreover, considering the carbon balance analysis that is obtained comparing the consumed amount of CH_4 to produced CO_2, a difference of less than 5% is found. Such result, coupled with the catalyst stability attributed to the absence of carbon (see Figure 5c), confirms the excellent capacity of the RP manganites for methane oxidation. As the water that is produced through the complete oxidation reaction is retained in a desiccator placed before the GC device, it was not possible to carry out any hydrogen or oxygen mass balance analysis.

The catalytic properties of A_2BO_4-type oxides with RP-type structure similar to $La_{0.25}Sr_{1.75}MnO_4$ catalyst of the present study, have been discussed in relation to the oxidation state of transition metal ions (B) and the oxygen non-stoichiometry. R. Karita *et al.* [28] found that the catalytic activity of $La_xSr_{2-x}MnO_4$ ($0.1 \leq x \leq 0.5$) for NO_x removal and CO oxidation, was low and high for the oxygen-deficient and oxygen-excess oxides, respectively. H. Zhong *et al*. [41] found that the catalytic activity of $LaSrMO_4$ (M= Mn, Fe, Co, Ni, Cu) for hexane oxidation is ordered from high to low activity as follow: $LaSrCoO_4$> $LaSrNiO_4$> $LaSrCuO_4$>$LaSrFeO_4$>$LaSrMnO_4$. They attributed part of this behavior to the presence of oxygen vacancies and mobile lattice oxygen.

Although reaction conditions are similar in catalytic tests, the result in the O_2 conversion in the second test, when O_2/CH_4= 0.089/0.094 (see Figure 5b), is different from the third test (stability), as observed in Figure 5c. This difference could be associated with a small deactivation caused by catalyst reduction at the beginning of reaction, then presenting a stable behavior. The stability behavior during 5h of reaction indicates that the catalyst does not promote the formation of carbonaceous deposits. It means that in oxygen conversion conditions,

the solid is in a dynamic equilibrium between the processes of reduction (when it delivers lattice oxygen atoms to the fuel) and re-oxidation (when it reintegrates oxygen atoms transferred from the gas phase).

Conclusions

$La_{0.25}Sr_{1.75}MnO_4$ has been synthesized by a modified Pechini method and the K_2NiF_4-type phase was obtained at a temperature of 1300°C in air. The material shows a reduction process in several steps with two hypotheses: (i) a first strong reduction peak of manganese from Mn^{4+} to Mn^{3+} below 600°C, followed by a second reduction peak to Mn^{2+}, weaker in intensity, between 600ºC and 800°C, before a high Mn^{3+} to Mn^{2+} reduction that leads to a decomposition of the RP manganite beyond 800°C. (ii) A first reduction from tetragonal *I*4/*mmm* symmetry to monoclinic $P2_1/c$ ordered oxygen deficient compound, as in $Sr_2MnO_{4-\delta}$ followed by a material decomposition. More work is needed, including a structural study as a function of temperature in reducing and oxidizing atmosphere, to clear up the observed behavior.

Catalytic evaluation of $La_{0.25}Sr_{1.75}MnO_4$ indicates that such material is selective towards total methane oxidation even in oxygen-deficient atmosphere, the catalytic activity being high for temperatures above 500°C. The catalytic behavior at 745°C is stable during the studied reaction time of 5h, without apparent formation of carbonaceous residues on the material. The RP manganite characteristics make it promising as anode material for intermediate temperature SOFC with operating temperatures below 800°C.

Acknowledgements

This work was developed with the financial support of (i) the Vice-Rectorship for Research and Extension of the Universidad Industrial de Santander, in the frame of the project # 1333 “Síntesis y caracterización de nuevos materiales pertenecientes al sistema $A_{2-x}RE_xMnO_4$ (A: Sr, Ca; RE: La, Nd, Gd) con potencial aplicación como ánodo en celdas de combustible de óxido sólido (SOFC)”, (ii) MINDEF (Argentina) with project PIDDEF N° 011/11 and (iii) CONICET and AANPCyT with project PICT 2013 1157. The authors are grateful to UIS´ laboratories of Microscopy and X-Ray in PTG Guatiguará for SEM and XRD measurements, and to Jorge Casanova for his collaboration with XRD measurements at CITEDEF.

References

[1] Zhu WZ, Deevi SC. A review on the status of anode materials for solid oxide fuel cells. Mater. Sci. Eng., A. 2003;362(1–2):228-39.

[2] Jiang S, Chan S. A review of anode materials development in solid oxide fuel cells. J. Mater. Sci. 2004;39(14):4405-39.

[3] Sun C, Stimming U. Recent anode advances in solid oxide fuel cells. J. Power Sources. 2007;171(2):247-60.

[4] Kee RJ, Zhu H, Goodwin DG. Solid-oxide fuel cells with hydrocarbon fuels. Proceedings of the Combustion Institute. 2005;30(2):2379-404.

[5] Steele BCH. Survey of materials selection for ceramic fuel cells II. Cathodes and anodes. Solid State Ionics. 1996;86–88, Part 2(0):1223-34.

[6] Ge X-M, Chan S-H, Liu Q-L, Sun Q. Solid Oxide Fuel Cell Anode Materials for Direct Hydrocarbon Utilization. Adv. Energy Mater. 2012;2(10):1156-81.

[7] Mukundan R, Brosha EL, Garzon FH. Sulfur Tolerant Anodes for SOFCs. Electrochem. Solid-State Lett. 2004;7(1):A5-A7.

[8] Cowin PI, Petit CTG, Lan R, Irvine JTS, Tao S. Recent Progress in the Development of Anode Materials for Solid Oxide Fuel Cells. Adv. Energy Mater. 2011;1(3):314-32.

[9] Hui S, Petric A. Electrical Properties of Yttrium-Doped Strontium Titanate under Reducing Conditions. J. Electrochem. Soc. 2002;149(1):J1-J10.

[10] Marina OA, Canfield NL, Stevenson JW. Thermal, electrical, and electrocatalytical properties of lanthanum-doped strontium titanate. Solid State Ionics. 2002;149(1–2):21-8.

[11] Canales-Vázquez J, Tao SW, Irvine JTS. Electrical properties in $La_2Sr_4Ti_6O_{19-\delta}$: a potential anode for high temperature fuel cells. Solid State Ionics. 2003;159(1–2):159-65.

[12] Hashimoto S, Kindermann L, Poulsen FW, Mogensen M. A study on the structural and electrical properties of lanthanum-doped strontium titanate prepared in air. J. Alloys Compd. 2005;397(1–2):245-9.

[13] Fu QX, Tietz F, Stöver D. $La_{0.4}Sr_{0.6}Ti_{1-x}Mn_xO_{3-\delta}$ Perovskites as Anode Materials for Solid Oxide Fuel Cells. J. Electrochem. Soc. 2006;153(4):D74-D83.

[14] Ovalle A, Ruiz-Morales JC, Canales-Vázquez J, Marrero-López D, Irvine JTS. Mn-substituted titanates as efficient anodes for direct methane SOFCs. Solid State Ionics. 2006;177(19–25):1997-2003.

[15] Ruiz-Morales JC, Canales-Vázquez J, Savaniu C, Marrero-López D, Zhou W, Irvine JTS. Disruption of extended defects in solid oxide fuel cell anodes for methane oxidation. Nature. 2006;439(7076):568-71.

[16] Miller DN, Irvine JTS. B-site doping of lanthanum strontium titanate for solid oxide fuel cell anodes. J. Power Sources. 2011;196(17):7323-7.

[17] Tarancon A, Skinner SJ, Chater RJ, Hernandez-Ramirez F, Kilner JA. Layered perovskites as promising cathodes for intermediate temperature solid oxide fuel cells. J. Mater. Chem. 2007;17(30):3175-81.

[18] Kharton VV, Yaremchenko AA, Shaula AL, Patrakeev MV, Naumovich EN, Logvinovich DI, et al. Transport properties and stability of Ni-containing mixed conductors with perovskite- and $K_2NiF_{4\text{-type}}$ structure. J. Solid State Chem. 2004;177(1):26-37.

[19] Lalanne C, Prosperi G, Bassat JM, Mauvy F, Fourcade S, Stevens P, *et al*. Neodymium-deficient nickelate oxide $Nd_{1.95}NiO_{4+\delta}$ as cathode material for anode-supported intermediate temperature solid oxide fuel cells. J. Power Sources. 2008;185(2):1218-24.

[20] Sayers R, Rieu M, Lenormand P, Ansart F, Kilner JA, Skinner SJ. Development of lanthanum nickelate as a cathode for use in intermediate temperature solid oxide fuel cells. Solid State Ionics. 2011;192(1):531-4.

[21] Le Flem G, Demazeau G, Hagenmuller P. Relations between structure and physical properties in $K_2NiF_{4\text{-type}}$ oxides. J. Solid State Chem. 1982;44(1):82-8.

[22] Bao W, Chen CH, Carter SA, Cheong SW. Electronic phase separation and charge ordering in $(Sr,La)_2MnO_4$: Indication of triplet bipolarons. Solid State Commun. 1996;98(1):55-9.

[23] Jennings AJ, Skinner SJ. Thermal stability and conduction properties of the $La_xSr_{2-x}FeO_{4+\delta}$ system. Solid State Ionics. 2002;152–153:663-7.

[24] Larochelle S, Mehta A, Lu L, Mang PK, Vajk OP, Kaneko N, *et al*. Structural and magnetic properties of the single-layer manganese oxide $La_{1-x}Sr_{1+x}MnO_4$. Phys. Rev. B: Condens. Matter. 2005;71(2):424-35.

[25] Li-Ping S, Qiang L, Li-Hua H, Hui Z, Guo-Ying Z, Nan L, *et al*. Synthesis and performance of $Sr_{1.5}La_xMnO_4$ as cathode materials for intermediate temperature solid oxide fuel cell. J. Power Sources. 2011;196(14):5835-9.

[26] Munnings CN, Skinner SJ, Amow G, Whitfield PS, Davidson IJ. Structure, stability and electrical properties of the $La_{2-x}Sr_xMnO_{4\pm\delta}$ solid solution series. Solid State Ionics. 2006;177(19–25):1849-53.

[27] Nie HW, Wen TL, Wang SR, Wang YS, Guth U, Vashook V. Preparation, thermal expansion, chemical compatibility, electrical conductivity and polarization of $A_{2-\alpha}A'_\alpha MO_4$ (A = Pr, Sm; A′ = Sr; M = Mn, Ni; α = 0.3, 0.6) as a new cathode for SOFC. Solid State Ionics. 2006;177(19–25):1929-32.

[28] Karita R, Kusaba H, Sasaki K, Teraoka Y. Synthesis, characterization and catalytic activity for NO–CO reaction of Pd–$(La, Sr)_2MnO_4$ system. Catal. Today. 2007;119(1–4):83-7.

[29] Karita R, Kusaba H, Sasaki K, Teraoka Y. Superiority of nitrate decomposition method for synthesis of $K_2NiF_{4\text{-type}}$ $La_xSr_{2-x}MnO_4$ catalysts. Catal. Today. 2007;126(3–4):471-5.

[30] Sakka S. Handbook of sol-gel science and technology. 1. Sol-gel processing: Springer Science & Business Media; 2005.

[31] Rodríguez-Carvajal J. Recent advances in magnetic structure determination by neutron powder diffraction. Physica B: Condensed Matter. 1993;192(1–2):55-69.

[32] Rodríguez-Carvajal J. Recent Developments of the Program FullProf. Commission on Powder Diffraction (IUCr) Newsletter. 2001;26:12-9.

[33] Berar J-F, Lelann P. Esd′s and estimated probable error obtained in Rietveld refinements with local correlations. J. Appl. Crystallogr. 1991;24(1):1-5.

[34] Monti DAM, Baiker A. Temperature-programmed reduction. Parametric sensitivity and estimation of kinetic parameters. J. Catal. 1983;83(2):323-35.

[35] Malet P, Caballero A. The selection of experimental conditions in temperature-programmed reduction experiments. J. Chem. Soc., Faraday Trans. 1. 1988;84(7):2369-75.

[36] Perego C, Peratello S. Experimental methods in catalytic kinetics. Catal. Today. 1999;52(2–3):133-45.

[37] Trambouze P. Countercurrent two-phase flow fixed bed catalytic reactors. Chem. Eng. Sci. 1990;45(8):2269-75.

[38] Weisz PB, Prater CD. Interpretation of Measurements in Experimental Catalysis. In: W.G. Frankenburg VIK, Rideal EK, editors.

Advances in Catalysis. Volume 6: Academic Press; 1954. p. 143-96.
[39] Frevel LK, Adams CE, Ruhberg LR. A fast search-match program for powder diffraction analysis. J. Appl. Crystallogr. 1976;9(3):199-204.
[40] Gorte RJ, Vohs JM. Nanostructured anodes for solid oxide fuel cells. Current Opinion in Colloid & Interface Science. 2009;14(4):236-44.
[41] ZHONG H, ZENG R. Structure of $LaSrMO_4$ (M = Mn, Fe, Co, Ni, Cu) and their catalytic properties in the total oxidation of hexane. J. Serb. Chem. Soc. 2006;71:1049–59.
[42] Ponce S, Peña MA, Fierro JLG. Surface properties and catalytic performance in methane combustion of Sr-substituted lanthanum manganites. Appl. Catal., B. 2000;24(3–4):193-205.
[43] Cimino S, Lisi L, Pirone R, Russo G, Turco M. Methane combustion on perovskites-based structured catalysts. Catal. Today. 2000;59(1–2):19-31.
[44] Porta P, De Rossi S, Faticanti M, Minelli G, Pettiti I, Lisi L, *et al*. Perovskite-Type Oxides: I. Structural, Magnetic, and Morphological Properties of $LaMn_{1-x}Cu_xO_3$ and $LaCo_{1-x}Cu_xO_3$ Solid Solutions with Large Surface Area. J. Solid State Chem. 1999;146(2):291-304.
[45] Rojas ML, Fierro JLG, Tejuca LG, Bell AT. Preparation and characterization of $LaMn_{1-x}CU_xO_{3+\lambda}$ perovskite oxides. J. Catal. 1990;124(1):41-51.
[46] Al Daroukh M, Vashook VV, Ullmann H, Tietz F, Arual Raj I. Oxides of the AMO_3 and $A_2MO_{4\text{-type}}$: structural stability, electrical conductivity and thermal expansion. Solid State Ionics. 2003;158(1–2):141-50.
[47] Broux T, Prestipino C, Bahout M, Hernandez O, Swain D, Paofai S, *et al*. Unprecedented High Solubility of Oxygen Interstitial Defects in $La_{1.2}Sr_{0.8}MnO_{4+\delta}$ up to $\delta \sim 0.42$ Revealed by In Situ High Temperature Neutron Powder Diffraction in Flowing O2. Chem. Mater. 2013;25(20):4053-63.
[48] Broux T, Bahout M, Hernandez O, Tonus F, Paofai S, Hansen T, *et al*. Reduction of Sr_2MnO_4 Investigated by High Temperature in Situ Neutron Powder Diffraction under Hydrogen Flow. Inorg. Chem. 2013;52(2):1009-17.